AIMS Mathematics, 11(4): 12108–12131.
DOI: 10.3934/math.2026497
Received: 22 January 2026
Revised: 14 April 2026
Accepted: 17 April 2026
Published: 29 April 2026

http://www.aimspress.com/journal/Math

Research article

Lorentzian construction of embankment-type ruled surfaces using the orthogonal modified frame in Minkowski 3-space

Mona Bin-Asfour[1], **Ghaliah Alhamzi**[1], **Emad Solouma**[1,*] **and Sayed Saber**[2]

[1] Department of Mathematics and Statistics, College of Science, Imam Mohammad Ibn Saud Islamic University (IMSIU), Riyadh, 11623, Saudi Arabia

[2] Department of Mathematics, Faculty of Science, Al-Baha University, Al-Baha 65779, Saudi Arabia

* **Correspondence:** Email: emmahmoud@imamu.edu.sa, emadms74@gmail.com.

Abstract: This study presents a new geometric formulation for constructing embankment–type ruled surfaces in the Lorentzian framework of Minkowski 3-space E_1^3, by means of the orthogonal modified frame (OMF). The OMF serves as an orthogonal moving frame that is fully compatible with the Minkowski metric, providing a consistent representation of the causal behavior of both spacelike and timelike curves. Within this framework, three distinct surface families are established namely, the OMF embankment surface, the OMF embankment–like surface, and the OMF tubembankment–like surface. Each class is developed together with its explicit parametric expression and associated geometric invariants. The corresponding first and second fundamental forms are derived, from which closed analytical expressions for the Gaussian curvature and mean curvature are obtained. These computations lead to precise differential conditions governing the developability and minimality of the generated surfaces. Representative examples illustrate the smooth curvature distribution and the Lorentzian metric consistency of the OMF–based models, demonstrating clear advantages over traditional Euclidean constructions. Overall, the proposed formulation offers an efficient and unified framework for analyzing and modeling ruled surfaces in Lorentzian geometry, with prospective applications in relativistic motion theory, geometric design, and computer-aided kinematic simulation.

Keywords: orthogonal modified frame; Minkowski 3-space; ruled surfaces; embankment surfaces; Lorentzian geometry; Gaussian curvature
Mathematics Subject Classification: 53A35, 53B30, 65D18

1. Introduction

Ruled and swept surfaces occupy a central position in differential geometry, serving as key models both in classical theory and in modern computational design. Among these, embankment-

type surfaces, generated as envelopes of a one-parameter family of cones whose vertices move along a spatial curve, arise naturally in engineering, kinematic modeling, and geometric processing. Traditionally, such surfaces have been examined within the Euclidean 3-space through the use of moving frames such as the Frenet, Darboux, or rotation minimizing frames, leading to well-known parametric representations, curvature relations, and classifications for specific generating (spine) curves.

When extended to the Lorentzian setting of Minkowski 3-space E_1^3, equipped with the metric signature $(+,+,-)$, the theory of ruled surfaces becomes considerably more intricate. The causal nature of both the base curve and the ruling, lines whether spacelike, timelike, or lightlike, must be consistently incorporated into the analysis. Within this geometric context, the recently introduced orthogonal modified frame (OMF) by Emad et al. [29] offers a torsion regulated, metric compatible orthonormal frame that remains coherent under Lorentzian inner products. This framework extends earlier approaches by preserving full orthogonality of frame vectors and providing a smooth analytic structure for the study of ruled surface invariants across varying causal types.

Modified frame constructions have recently attracted considerable attention across a variety of geometric settings, including Euclidean, Galilean, and Lorentzian spaces, due to their flexibility and robustness in both geometric modeling and kinematic analysis. In Euclidean geometry, alternative moving frames such as the Bishop frame and its generalizations are widely employed in applications requiring smooth frame evolution, particularly in computer-aided design and motion interpolation, where classical Frenet frames may fail at points of vanishing curvature. Recent developments have further extended these ideas to dynamical settings, where the evolution of such frames is governed by differential equations describing inextensible flows and kinematic constraints [12].

In Galilean geometry, where the metric degenerates and the classical Frenet apparatus is not globally defined, several alternative frame formulations such as quasi-frames and modified Bishop-type frames have been introduced to overcome these limitations. These constructions provide consistent tools for analyzing curve behavior and associated surfaces in non-relativistic settings. For instance, recent studies have shown that quasi-frame structures allow the characterization of curves and their higher-order kinematic quantities in Galilean space, even in the presence of degeneracies [10]. Moreover, the use of modified Bishop frames has been successfully applied to the study of translation and ruled surfaces in Galilean space, highlighting their effectiveness in curvature analysis and geometric design [20]. In parallel, generalized Galilean transformations and rotations have been investigated to better understand motion and frame behavior under non-Euclidean scalar products [6].

From a kinematic viewpoint, modified frames admit a natural interpretation in terms of motion along curves. The tangent vector describes the instantaneous direction of velocity, while the associated normal and binormal vectors capture acceleration and directional variation. The evolution equations governing these frames encode the local rotational behavior of the system and can be interpreted in terms of angular velocity and frame transport, which are essential in applications such as robotics, animation, and trajectory optimization. Recent works on the evolution of Bishop-type frames in Lorentzian settings further demonstrate how such formulations can describe inextensible curve flows and dynamic geometric behavior [12].

It is also important to emphasize that the qualitative behavior of these frames depends strongly on the ambient metric signature. In Euclidean space, frame transformations are governed by circular rotations, whereas in Lorentzian geometry, they are described by hyperbolic rotations involving cosh

and sinh, reflecting the causal structure of Minkowski space. In contrast, Galilean geometry exhibits fundamentally different transformation properties due to its degenerate metric, leading to distinct geometric and kinematic characteristics. These distinctions underline the importance of adapting frame constructions to the underlying geometry. In this context, the OMF adopted in the present work provides a consistent and geometrically compatible framework for the analysis of ruled surfaces in Lorentzian space, while maintaining conceptual connections with recent developments in Euclidean and Galilean geometries.

1.1. Cross-metric structure of the OMF and its kinematic significance

The geometric behavior of moving frames is intrinsically linked to the metric structure of the ambient space. To highlight the scope of the OMF, we examine its formulation across Euclidean space E^3, Minkowski space E_1^3, and Galilean space G^3. Each setting induces distinct geometric and kinematic characteristics that influence both frame evolution and the associated ruled surface constructions.

Galilean space G^3 is characterized by a degenerate metric, which prevents the direct application of classical Frenet-type frames. Consequently, alternative constructions such as quasi-frames and modified Bishop-type frames are employed to describe curve geometry in a consistent manner. These adapted frames allow the definition of curvature-like invariants and support the construction of ruled and translation surfaces despite the lack of a fully non-degenerate inner product.

Recent studies have demonstrated the effectiveness of such approaches in analyzing curve behavior and surface generation in Galilean geometry. In particular, the use of quasi-frame structures enables a consistent treatment of curvature and torsion analogues, even under degeneracy conditions [9, 23]. Unlike the circular behavior observed in Euclidean space or the hyperbolic behavior in Minkowski space, Galilean geometry typically yields parabolic or linear structural patterns.

From a kinematic perspective, the OMF provides a natural framework for describing motion along a curve $\beta(\sigma)$. The tangent vector

$$\mathbf{v}(\sigma) = \frac{d\beta}{d\sigma},$$

represents the instantaneous velocity, while the acceleration is given by

$$\mathbf{a}(\sigma) = \frac{d^2\beta}{d\sigma^2}.$$

The evolution of the OMF triad $\{\mathbf{T}, \mathbf{N}, \mathbf{B}\}$ is governed by

$$\dot{\mathbf{T}} = \mathbf{N}, \quad \dot{\mathbf{N}} = -\varepsilon\kappa^2\,\mathbf{T} + \left(\frac{\dot{\kappa}}{\kappa}\right)\mathbf{N} + \tau\,\mathbf{B}, \quad \dot{\mathbf{B}} = \tau\,\mathbf{N} + \left(\frac{\dot{\kappa}}{\kappa}\right)\mathbf{B},$$

which can be expressed in matrix form as

$$\dot{\mathrm{R}}_{\mathrm{OMF}} = \Omega_{\mathrm{OMF}}\,\mathrm{R}_{\mathrm{OMF}}.$$

The matrix Ω_{OMF} represents the instantaneous rotational behavior of the frame and can be interpreted as a generalized angular velocity operator. Its physical and geometric meaning depends on the metric structure:

- In Euclidean space, it corresponds to classical angular velocity.

- In Minkowski space, it generates Lorentzian rotations (boosts).
- In Galilean space, it reduces to a degenerate operator describing constrained motion.

Such interpretations have been explored in recent works on geometric flows and frame dynamics, where modified frames are applied to model inextensible motions and trajectory evolution [7, 19].

The behavior of an OMF-based ruled surface varies significantly depending on the ambient metric. This is summarized in the following comparison (see Table 1):

Table 1. Comparative overview of metric structure, transformation behavior, frame properties, kinematics, and surface section geometry of the OMF across Euclidean, Minkowski, and Galilean spaces.

Feature	Euclidean E^3	Minkowski E_1^3	Galilean G^3
E metric structure	Positive definite	Indefinite $(+,+,-)$	Degenerate
Transformation type	Circular $(\cos, \sin)$	Hyperbolic $(\cosh, \sinh)$	Linear / parabolic
Frame structure	Orthonormal	Lorentz-orthonormal	Quasi-frame
Kinematics	Classical rotation	Lorentz boosts	Constrained motion
Surface sections	Circular	Hyperbolic	Parabolic

This comparison shows that the OMF is a metric-dependent construction whose interpretation varies across geometries while preserving a unified analytical structure. Consequently, this cross-metric viewpoint reinforces the effectiveness of the OMF in geometric design, relativistic modeling, and kinematic applications.

In recent years, the study of ruled surfaces under Lorentzian and other generalized metrics has attracted renewed attention due to both theoretical developments and practical motivations. For example, Al Ahmady et al. [1] investigated the classification of constant axis timelike-ruled surfaces in Minkowski 3-space, while Silva and Silva [25] explored homothetic self-similar ruled surfaces arising from the inverse mean curvature flow in Lorentz-Minkowski geometry. Furthermore, [8, 11, 29] established a unified analytical framework for Lorentzian-ruled surfaces using the OMF, yielding new curvature characterizations and generalized developability criteria. These contributions underscore the wide applicability of ruled surface models beyond purely theoretical geometry extending into relativistic kinematics, wave front evolution, and Lorentzian architectural structures [24, 26, 27]. In engineering practice, formulations based on Lorentzian ruled surfaces and frame-based methods have been employed in geometric modeling, stability analysis, and computational frameworks related to advanced applications [3, 13, 21].

Alongside these application-oriented advances, the mathematical structure of ruled surfaces has been enriched by numerous methodological generalizations. The Darboux frame-based analysis of embankment and tubembankment surfaces developed by Kocakusakli [14] has been further extended through alternative frame methods adapted to Minkowski geometry. Notably, the split quaternion operator formulation for ruled surfaces [18, 32] and the use of modified Lorentzian frames for surface evolution [2, 5, 30] have provided new computational paradigms with enhanced analytic transparency and numerical robustness. Additionally, Li et al. [15] studied the singularity structures of developable timelike surfaces, revealing further geometric depth in Lorentzian–ruled configurations. Building upon

these developments, the present paper revisits embankment and tubembankment-type surfaces through the OMF, deriving explicit parametric equations, curvature invariants, and conditions for developability adapted to the Minkowski 3-space E_1^3.

The central objective of this research is to extend the OMF framework to the geometry of embankment-type ruled surfaces in Lorentzian 3-space, derive their parametric forms and differential invariants, and compare the resulting geometry with the classical Euclidean analogues. Through this approach, the paper aims to contribute both to the theoretical understanding of ruled surfaces under Lorentzian metrics and to the applied modeling techniques relevant in geometric design, motion simulation, and relativistic mechanics.

The structure of the paper is organized as follows. Section 2 reviews the necessary preliminaries on Minkowski 3-space and introduces the OMF. Section 3 constructs the parametric forms of OMF–based embankment surfaces and presents their quaternionic and matrix representations. In Section 4, the first and second fundamental forms are derived together with the Gaussian and mean curvatures, and analytical criteria for minimality and developability are obtained. Section 5 provides representative examples illustrating curvature evolution for specific spine curves. Finally, Section 6 summarizes the main findings and outlines directions for future investigation.

2. Preliminaries

Let E_1^3 denote the three-dimensional Minkowski space equipped with the Lorentzian metric

$$\mathfrak{I} = d\varsigma_1^2 + d\varsigma_2^2 - d\varsigma_3^2,$$

where $(\varsigma_1, \varsigma_2, \varsigma_3) \in \mathrm{E}_1^3$. For any vector $\beta \in \mathrm{E}_1^3$, its causal character is determined by

$$\mathfrak{I}(\beta,\beta) > 0 \text{ or } \beta = 0 \Rightarrow \text{spacelike}, \quad \mathfrak{I}(\beta,\beta) < 0 \Rightarrow \text{timelike}, \quad \mathfrak{I}(\beta,\beta) = 0,\ \beta \neq 0 \Rightarrow \text{null}.$$

A smooth curve $\beta = \beta(\sigma)$ is called spacelike, timelike, or null according to the causal type of its tangent vector $\beta'(\sigma)$ [22, 28].

Let $\beta = \beta(\sigma)$ be a regular spacelike curve in E_1^3. Its Frenet trihedron $\{t(\sigma), n(\sigma), b(\sigma)\}$ satisfies the Lorentzian Frenet-Serret system [16, 31]:

$$\begin{aligned} t_\sigma(\sigma) &= \kappa(\sigma)\, n(\sigma), \\ n_\sigma(\sigma) &= -\varepsilon\, \kappa(\sigma)\, t(\sigma) + \tau(\sigma)\, b(\sigma), \\ b_\sigma(\sigma) &= \tau(\sigma)\, n(\sigma), \end{aligned} \tag{2.1}$$

where the Lorentzian inner products satisfy

$$\mathfrak{I}(t,t) = 1, \quad \mathfrak{I}(n,n) = \varepsilon, \quad \mathfrak{I}(b,b) = -\varepsilon, \quad \mathfrak{I}(t,n) = \mathfrak{I}(t,b) = \mathfrak{I}(n,b) = 0.$$

Here, $\varepsilon = 1$ corresponds to a spacelike curve of the first kind, while $\varepsilon = -1$ indicates a spacelike curve of the second kind.

Suppose that $\beta(\sigma)$ is an analytic spacelike curve whose curvature $\kappa(\sigma)$ is nonzero except at isolated points. Then, the OMF $\{\mathbf{T}(\sigma), \mathbf{N}(\sigma), \mathbf{B}(\sigma)\}$ is defined as [8, 29]

$$\begin{aligned}
\mathbf{T}_\sigma(\sigma) &= \mathbf{N}(\sigma),\\
\mathbf{N}_\sigma(\sigma) &= -\varepsilon\,\kappa^2(\sigma)\,\mathbf{T}(\sigma) + \left(\frac{\kappa_\sigma(\sigma)}{\kappa(\sigma)}\right)\mathbf{N}(\sigma) + \tau(\sigma)\,\mathbf{B}(\sigma),\\
\mathbf{B}_\sigma(\sigma) &= \tau(\sigma)\,\mathbf{N}(\sigma) + \left(\frac{\kappa_\sigma(\sigma)}{\kappa(\sigma)}\right)\mathbf{B}(\sigma).
\end{aligned} \tag{2.2}$$

The frame vectors satisfy the orthogonality conditions

$$\Im(\mathbf{T},\mathbf{T}) = 1, \quad \Im(\mathbf{N},\mathbf{N}) = \varepsilon\kappa^2, \quad \Im(\mathbf{B},\mathbf{B}) = -\varepsilon\kappa^2, \quad \Im(\mathbf{T},\mathbf{N}) = \Im(\mathbf{T},\mathbf{B}) = \Im(\mathbf{N},\mathbf{B}) = 0.$$

Unlike the classical Frenet frame, the OMF remains stable near torsion singularities and is particularly well suited for analytical and numerical modeling of surfaces.

Consider now a spacelike ruled surface parameterized by

$$\Phi(\sigma,\theta) = \beta(\sigma) + \theta\,\mathbf{d}(\sigma), \qquad \mathbf{d}(\sigma) = \cosh\lambda(\sigma)\,\mathbf{N}(\sigma) + \sinh\lambda(\sigma)\,\mathbf{B}(\sigma), \tag{2.3}$$

with tangent vectors

$$\Phi_\sigma = \frac{\partial\Phi}{\partial\sigma}, \qquad \Phi_\theta = \frac{\partial\Phi}{\partial\theta}.$$

The coefficients of the first fundamental form are given by

$$\mathrm{E} = \Im(\Phi_\sigma,\Phi_\sigma), \qquad \mathrm{F} = \Im(\Phi_\sigma,\Phi_\theta), \qquad \mathrm{G} = \Im(\Phi_\theta,\Phi_\theta),$$

and for a spacelike surface one has $\mathrm{EG} - \mathrm{F}^2 > 0$. The unit normal vector is

$$\mathbf{n} = \frac{\Phi_\sigma \times \Phi_\theta}{\|\Phi_\sigma \times \Phi_\theta\|},$$

and the coefficients of the second fundamental form are

$$\mathrm{L} = \Im(\Phi_{\sigma\sigma},\mathbf{n}), \quad \mathrm{M} = \Im(\Phi_{\sigma\theta},\mathbf{n}), \quad \mathrm{N} = \Im(\Phi_{\theta\theta},\mathbf{n}).$$

Consequently, the Gaussian and mean curvatures of $\Phi(\sigma,\theta)$ are expressed as

$$\mathrm{K}_\Phi = \frac{\mathrm{LN} - \mathrm{M}^2}{\mathrm{EG} - \mathrm{F}^2}, \qquad \mathrm{H}_\Phi = \frac{\mathrm{EN} + \mathrm{GL} - 2\mathrm{FM}}{2(\mathrm{EG} - \mathrm{F}^2)}. \tag{2.4}$$

A ruled surface is developable when $\mathrm{K}_\Phi = 0$ and minimal when $\mathrm{H}_\Phi = 0$ [4, 16]. These curvature relations serve as the analytical foundation for the OMF-based embankment and tubembankment surfaces introduced in the subsequent sections.

In Minkowski space E_1^3, the quaternionic algebra can be generalized by adopting split quaternions, which provide a natural representation for Lorentzian rotations and boosts. A split quaternion $\mathrm{Q} = (q_0, q_1, q_2, q_3)$ satisfies the Lorentzian norm condition

$$\langle \mathrm{Q}, \mathrm{Q} \rangle = q_0^2 + q_1^2 - q_2^2 - q_3^2.$$

For any vector $w = (w_1, w_2, w_3) \in \mathrm{E}_1^3$, its pure quaternion representation is

$$\mathrm{Q}_w = (0, w_1, w_2, w_3),$$

and the Lorentzian rotation of w is defined by

$$\mathrm{Q}'_w = \mathrm{Q}\,\mathrm{Q}_w\,\mathrm{Q}^*, \tag{2.5}$$

where $mathrmQ^* = (q_0, -q_1, -q_2, -q_3)$. This transformation preserves the Minkowski inner product, thereby representing a Lorentz-orthogonal motion. If the OMF triad $\{\mathbf{T}, \mathbf{N}, \mathbf{B}\}$ is represented by the quaternion set $\{\mathrm{Q}_\mathbf{T}, \mathrm{Q}_\mathbf{N}, \mathrm{Q}_\mathbf{B}\}$, then the frame equations (2.2) admit the quaternionic differential form

$$\dot{\mathrm{Q}}_\mathbf{T} = \mathrm{Q}_\mathbf{N}, \quad \dot{\mathrm{Q}}_\mathbf{N} = -\varepsilon\,\kappa^2 \mathrm{Q}_\mathbf{T} + \left(\frac{\dot{\kappa}}{\kappa}\right)\mathrm{Q}_\mathbf{N} + \tau \mathrm{Q}_\mathbf{B}, \quad \dot{\mathrm{Q}}_\mathbf{B} = \tau \mathrm{Q}_\mathbf{N} + \left(\frac{\dot{\kappa}}{\kappa}\right)\mathrm{Q}_\mathbf{B}.$$

Hence, the evolution of the OMF trihedron in E_1^3 can be interpreted as a Lorentz-orthogonal quaternion flow preserving frame orthogonality under the indefinite metric [17, 29].

The orthogonal transformation between the global Minkowski basis $\{e_1, e_2, e_3\}$ and the local OMF basis $\{\mathbf{T}, \mathbf{N}, \mathbf{B}\}$ is expressed by the Lorentz rotation matrix

$$\mathbf{R}_{\mathrm{OMF}}(\sigma) = \begin{bmatrix} \mathbf{T}_1 & \mathbf{N}_1 & \mathbf{B}_1 \\ \mathbf{T}_2 & \mathbf{N}_2 & \mathbf{B}_2 \\ \mathbf{T}_3 & \mathbf{N}_3 & \mathbf{B}_3 \end{bmatrix}, \tag{2.6}$$

which satisfies

$$\mathbf{R}_{\mathrm{OMF}}^{\mathbf{T}}\,\mathbf{I}_1\,\mathbf{R}_{\mathrm{OMF}} = \mathbf{I}_1, \qquad \mathbf{I}_1 = \mathrm{diag}(1, 1, -1),$$

ensuring that $\mathbf{R}_{\mathrm{OMF}} \in \mathrm{O}(2, 1)$, the Lorentz group of orthogonal transformations in E_1^3. The instantaneous rotation rate of the frame is governed by

$$\dot{\mathbf{R}}_{\mathrm{OMF}} = \mathbf{\Omega}_{\mathrm{OMF}}\,\mathbf{R}_{\mathrm{OMF}},$$

where $\mathbf{\Omega}_{\mathrm{OMF}}$ is a Lorentz-skew matrix given by

$$\mathbf{\Omega}_{\mathrm{OMF}} = \begin{bmatrix} 0 & \kappa^2 & 0 \\ -\varepsilon\,\kappa^2 & \dfrac{\dot{\kappa}}{\kappa} & \tau \\ 0 & \tau & \dfrac{\dot{\kappa}}{\kappa} \end{bmatrix}.$$

This representation facilitates efficient symbolic and numerical computation of OMF-based surfaces in Lorentzian geometric modeling [17, 18].

Finally, consider a one-parameter family of homothetic motions $\mathcal{H}(\sigma)$ in E_1^3, defined by a positive scale function $\mu(\sigma) > 0$, a Lorentz rotation matrix $\mathbf{R}_{\mathrm{OMF}}(\sigma)$, and a translation vector $\mathbf{P}(\sigma) \in \mathrm{E}_1^3$:

$$\mathcal{H}(\sigma) = \mu(\sigma)\,\mathbf{R}_{\mathrm{OMF}}(\sigma)\,\mathbf{x} + \mathbf{P}(\sigma). \tag{2.7}$$

This transformation preserves causal type and generalizes classical Euclidean homotheties to the Lorentzian metric. Applying $\mathcal{H}(\sigma)$ to the base curve $\beta(\sigma)$ yields a one-parameter family of OMF-based ruled surfaces,

$$\Phi(\sigma, \theta) = \mu(\sigma)\,\mathbf{R}_{\mathrm{OMF}}(\sigma)[\beta(\sigma) + \theta\,\mathbf{d}(\sigma)] + \mathbf{P}(\sigma),$$

where $\mathbf{d}(\sigma)$ is the ruling vector given in (2.3). Here, $\mu(\sigma)$ governs isotropic scaling, and $\mathbf{R}_{\text{OMF}}$ defines the Lorentzian rotational behavior. This unified framework enables the construction of dynamically evolving OMF embankment, embankment-like, and tubembankment-like surfaces in E_1^3 under continuous Lorentz-orthogonal motion [1, 18].

Remark 2.1. *The Frenet frame becomes undefined at points where the curvature vanishes, leading to instability in geometric constructions. In contrast, the OMF remains well-defined and preserves orthogonality along the curve, making it more suitable for applications requiring stable frame fields.*

3. Parametric construction of OMF embankment surfaces via envelope mechanisms

In this section, we construct the parametric formulation of embankment-type ruled surfaces generated with respect to the OMF in the Lorentzian space E_1^3. This approach generalizes the Euclidean rotation, minimizing surface generation by utilizing the Minkowski inner product

$$\mathfrak{I}(x, y) = x_1y_1 + x_2y_2 - x_3y_3,$$

together with the OMF triad $\{\mathbf{T}, \mathbf{N}, \mathbf{B}\}$ described in (2.2). The orthogonality of this frame with respect to the Lorentzian metric ensures stability about the tangent vector and allows a consistent treatment of Lorentzian cone envelopes associated with spacelike base curves.

Let $\beta(\sigma)$ denote a smooth spacelike curve parameterized by the arc length σ in E_1^3. At each point $\beta(\sigma)$, consider a one-parameter family of right Lorentzian cones whose vertices coincide with $\beta(\sigma)$, whose axes are directed along $\mathbf{T}(\sigma)$, and whose semi-angle with the axis equals $\arctan\left(\frac{1}{n}\right)$, where $n > 0$ is a constant slope parameter. The envelope of this family defines the corresponding OMF embankment surface.

Definition 3.1. Let $\beta : I \subset \mathbb{R} \to \mathrm{E}_1^3$ be a regular spacelike curve equipped with the OMF $\{\mathbf{T}, \mathbf{N}, \mathbf{B}\}$ and slope parameter $n > 0$. Then the OMF embankment surface associated with β is given by

$$\Gamma_\beta^{\text{OMF}}(\sigma, \phi) = \beta(\sigma) + \delta_1(\sigma, \phi)\,\mathbf{T}(\sigma) + \delta_2(\sigma, \phi)\,\mathbf{N}(\sigma) + \delta_3(\sigma, \phi)\,\mathbf{B}(\sigma), \tag{3.1}$$

where the scalar fields $\delta_1, \delta_2, \delta_3$ satisfy the envelope conditions of the Lorentzian cone family determined by the slope n.

The implicit expression of the right Lorentzian cone with vertex $\beta(\sigma)$ and axis $\mathbf{T}(\sigma)$ reads

$$f(\mathbf{r}, \sigma) = \|\mathbf{r} - \beta(\sigma)\|^2 - \frac{1}{1 + n^2}\,\mathfrak{I}(\mathbf{r} - \beta(\sigma), \mathbf{T}(\sigma))^2 = 0. \tag{3.2}$$

The envelope of the cone family is defined by the system

$$\begin{cases} f(\mathbf{r}, \sigma) = 0, \\ \dfrac{\partial f(\mathbf{r}, \sigma)}{\partial \sigma} = 0. \end{cases} \tag{3.3}$$

Theorem 3.1. *Let $\beta(\sigma)$ be a spacelike curve in E_1^3 endowed with the OMF $\{\mathbf{T}, \mathbf{N}, \mathbf{B}\}$. Let $n > 0$, and let $\rho(\sigma, \phi)$ be a sufficiently smooth function such that*

$$1 - (1 + n^2)\,\rho_\sigma^2 > 0.$$

Then the envelope of the cone family (3.2) *defines a regular OMF embankment surface given by*

$$\begin{aligned}\Gamma_\beta^{\mathrm{OMF}}(\sigma,\phi) &= \beta(\sigma) - (1+n^2)\,\rho(\sigma,\phi)\,\rho_\sigma\,\mathbf{T}(\sigma)\\ &\pm \sqrt{1+n^2}\,\rho(\sigma,\phi)\sqrt{1-(1+n^2)\,\rho_\sigma^2}\,(\cosh\phi\,\mathbf{N}(\sigma)+\sinh\phi\,\mathbf{B}(\sigma)),\end{aligned} \tag{3.4}$$

where $\rho(\sigma,\phi)$ represents the radial displacement of the generatrix.

Moreover, the condition $1-(1+n^2)\,\rho_\sigma^2 > 0$ ensures that the parametrization is real-valued and non-degenerate. If $1-(1+n^2)\,\rho_\sigma^2 = 0$, the surface becomes singular, while if $1-(1+n^2)\,\rho_\sigma^2 < 0$, the parametrization yields non-real (imaginary) points and thus does not define a valid surface in E_1^3.

Proof. Writing $\mathbf{r}-\beta(\sigma) = \delta_1\mathbf{T}+\delta_2\mathbf{N}+\delta_3\mathbf{B}$ and substituting into (3.2), using $\Im(\mathbf{T},\mathbf{T}) = 1$, $\Im(\mathbf{N},\mathbf{N}) = 1$, and $\Im(\mathbf{B},\mathbf{B}) = -1$, one obtains

$$(1+n^2)(\delta_2^2-\delta_3^2) - n^2\delta_1^2 = 0.$$

Thus, $\delta_1^2 = \left(\frac{1+n^2}{n^2}\right)\left(\delta_2^2-\delta_3^2\right)$. Letting $\delta_2 = \rho\cosh\phi$ and $\delta_3 = \rho\sinh\phi$ implies $\delta_2^2-\delta_3^2 = \rho^2$. Differentiating (3.2) with respect to σ, substituting $\mathbf{T}' = \kappa^2\mathbf{N}$ from (2.2), and enforcing the envelope condition (3.3) yields $\delta_1 = -(1+n^2)\rho\rho_\sigma$. Inserting these results into (3.1) gives (3.4). □

Proposition 3.1. *Define the unit split quaternion*

$$\Lambda(\sigma,\phi) = \cosh\left(\frac{\phi}{2}\right) + \sinh\left(\frac{\phi}{2}\right)\mathbf{T}(\sigma),$$

which represents a hyperbolic rotation about $\mathbf{T}(\sigma)$ through angle ϕ such that

$$\|\Lambda(\sigma,\phi)\|^2 = \cosh^2\left(\frac{\phi}{2}\right) - \sinh^2\left(\frac{\phi}{2}\right) = 1.$$

Thus, $\Lambda(\sigma,\phi)$ is properly normalized in the split quaternion sense and the surface (3.4) *can equivalently be expressed as*

$$\Gamma_\beta^{\mathrm{OMF}}(\sigma,\phi) = \beta(\sigma) - (1+n^2)\,\rho\,\rho_\sigma\,\mathbf{T}(\sigma) \pm \sqrt{1+n^2}\,\rho\sqrt{1-(1+n^2)\,\rho_\sigma^2}\,(\Lambda\,\mathbf{N}\,\Lambda^{-1}). \tag{3.5}$$

Proof. For any pure quaternion $\upsilon \in \mathrm{E}_1^3$, the Lorentzian rotation by Λ is $\upsilon' = \Lambda\,\upsilon\,\Lambda^{-1}$. Since $\mathbf{N}$ and $\mathbf{B}$ form the orthogonal complement of $\mathbf{T}$, we have

$$\Lambda\,\mathbf{N}\,\Lambda^{-1} = \cosh\phi\,\mathbf{N} + \sinh\phi\,\mathbf{B}. \tag{3.6}$$

Substituting (3.6) into (3.4) directly yields (3.5). □

Corollary 3.1. *Let $Q_\Lambda \in O(2,1)$ denote the Lorentz-orthogonal matrix corresponding to $\Lambda(\sigma,\phi)$, and let $h(\sigma) = \sqrt{1+n^2}\,\rho(\sigma,\phi)$. Then the OMF embankment surface can be expressed as*

$$\Gamma_\beta^{\mathrm{OMF}}(\sigma,\phi) = \beta(\sigma) - (1+n^2)\,\rho\,\rho_\sigma\,\mathbf{T}(\sigma) \pm h(\sigma)\sqrt{1-(1+n^2)\,\rho_\sigma^2}\,Q_\Lambda\,\mathbf{N}(\sigma). \tag{3.7}$$

Remark 3.1. *Relations* (3.5) *and* (3.7) *demonstrate that the OMF embankment surface represents a Lorentz homothetic transformation of the normal vector $\mathbf{N}(\sigma)$, where the hyperbolic rotation is described by the split quaternion $\Lambda(\sigma,\phi)$ and the isotropic dilation is governed by $h(\sigma)$. This concise representation is well suited for Lorentzian surface modeling, geometric visualization, and computer-aided design applications.*

3.1. Special configurations

(1) If the torsion satisfies $\tau(\sigma) = 0$, the parameter $\phi(\sigma)$ remains constant, and the OMF reduces to the classical Frenet frame. In this case, expression (3.4) collapses to the Euclidean embankment surface described in [14].

(2) If $\rho(\sigma, \phi) = c > 0$ is constant, then the surface reduces to a tubembankment-like surface of the form

$$\Gamma_{\mathbf{T}}^{\mathrm{OMF}}(\sigma, \phi) = \beta(\sigma) \pm c\sqrt{1+n^2}\,(\cosh\phi\,\mathbf{N}(\sigma) + \sinh\phi\,\mathbf{B}(\sigma)),$$

whose curvature and geometric features are analyzed in Section 4.

Corollary 3.2. *For a fixed σ_0, the parameter curve $\phi \mapsto \Gamma_{\beta}^{\mathrm{OMF}}(\sigma_0, \phi)$ forms a hyperbolic cross-section in the Minkowski plane orthogonal to $\mathbf{T}(\sigma_0)$, centered at*

$$\beta(\sigma_0) - (1+n^2)\,\rho(\sigma_0, \phi)\,\rho_\sigma(\sigma_0, \phi)\,\mathbf{T}(\sigma_0),$$

with Lorentzian radius

$$\mathrm{R}(\sigma_0, \phi) = \sqrt{1+n^2}\,\rho(\sigma_0, \phi)\sqrt{1-(1+n^2)\,\rho_\sigma(\sigma_0, \phi)^2}.$$

4. Extended OMF embankment families and their differential structures

In this section, we examine the principal differential geometric quantities associated with the OMF embankment surface (3.4) introduced in Theorem 3.1. Our aim is to derive explicit formulas for the first and second fundamental forms, together with the Gaussian and mean curvatures, in the Lorentzian ambient space E_1^3. Through the OMF, one can effectively capture how the Lorentzian metric influences curvature and developability, while maintaining a formulation that remains free of torsional or rotational singularities. The analysis clarifies both the intrinsic and extrinsic geometry of the OMF embankment surface and allows for direct comparison with analogous formulations based on Darboux or rotation minimizing frames. This highlights the benefits of the OMF representation for ensuring curvature continuity and numerical robustness in relativistic or geometric modeling applications.

Substitute the OMF relations

$$\mathbf{T}' = \mathbf{N}, \quad \mathbf{N}_\sigma = -\varepsilon\kappa^2\mathbf{T} + \frac{\kappa_\sigma}{\kappa}\mathbf{N} + \tau\mathbf{B}, \quad \mathbf{B}_\sigma = \tau\mathbf{N} + \frac{\kappa_\sigma}{\kappa}\mathbf{B},$$

into (4.1).

Differentiating (3.4) with respect to the parameters σ and ϕ yields the tangent vectors:

$$\begin{aligned} \Gamma_\sigma^{\mathrm{OMF}} &= \Gamma_\sigma^{\mathrm{OMF}} = a_T\mathbf{T} + a_N\mathbf{N} + a_B\mathbf{B}, \\ \Gamma_\phi^{\mathrm{OMF}} &= \pm\sqrt{1+n^2}\,\rho\sqrt{1-(1+n^2)\,\rho_\sigma^2}(\sinh\phi\,\mathbf{N} + \cosh\phi\,\mathbf{B}), \end{aligned} \tag{4.1}$$

where

$$a_T = 1 - (1+n^2)(\rho_\sigma^2 + \rho\rho_{\sigma\sigma}) \mp \varepsilon\sqrt{1+n^2}\,\rho\sqrt{1-(1+n^2)\rho_\sigma^2}\,\kappa^2(\cosh\phi),$$

$$a_N = -(1+n^2)\rho\rho_\sigma \pm \sqrt{1+n^2}\left[\rho_\sigma\sqrt{1-(1+n^2)\rho_\sigma^2} - \frac{(1+n^2)\rho\rho_\sigma\rho_{\sigma\sigma}}{\sqrt{1-(1+n^2)\rho_\sigma^2}}\right]\cosh\phi$$

$$\pm\ \sqrt{1+n^2}\,\rho\sqrt{1-(1+n^2)\rho_\sigma^2}\left(\frac{\kappa_\sigma}{\kappa}\cosh\phi+\tau\sinh\phi\right),$$

$$a_B = \pm\sqrt{1+n^2}\left[\rho_\sigma\sqrt{1-(1+n^2)\rho_\sigma^2}-\frac{(1+n^2)\rho\rho_\sigma\rho_{\sigma\sigma}}{\sqrt{1-(1+n^2)\rho_\sigma^2}}\right]\sinh\phi$$
$$\pm\ \sqrt{1+n^2}\,\rho\sqrt{1-(1+n^2)\rho_\sigma^2}\left(\tau\cosh\phi+\frac{\kappa_\sigma}{\kappa}\sinh\phi\right).$$

Using the orthogonality relations of the OMF,

$$\langle\mathbf{T},\mathbf{T}\rangle = 1,\quad \langle\mathbf{N},\mathbf{N}\rangle = \varepsilon\kappa^2,\quad \langle\mathbf{B},\mathbf{B}\rangle = -\varepsilon\kappa^2,$$

and $\langle\mathbf{T},\mathbf{N}\rangle = \langle\mathbf{T},\mathbf{B}\rangle = \langle\mathbf{N},\mathbf{B}\rangle = 0$, we obtain

$$\begin{aligned}
\mathrm{E}_\Gamma^{\mathrm{OMF}} &= \Im(\Gamma_\sigma^{\mathrm{OMF}},\Gamma_\sigma^{\mathrm{OMF}}) = a_T^2+\varepsilon\kappa^2(a_N^2-a_B^2),\\
\mathrm{F}_\Gamma^{\mathrm{OMF}} &= \Im(\Gamma_\sigma^{\mathrm{OMF}},\Gamma_\phi^{\mathrm{OMF}}),\quad \mathrm{G}_\Gamma^{\mathrm{OMF}} = \Im(\Gamma_\phi^{\mathrm{OMF}},\Gamma_\phi^{\mathrm{OMF}}).
\end{aligned}\tag{4.2}$$

After simplification, this reduces to

$$\begin{aligned}
\mathrm{E}_\Gamma^{\mathrm{OMF}} &= 1+(1+n^2)^2(\rho\rho_{\sigma\sigma}+\rho_\sigma^2)^2+(1+n^2)\,\rho^2\rho_\sigma^2(\kappa^4+\tau^2),\\
\mathrm{F}_\Gamma^{\mathrm{OMF}} &= 0,\\
\mathrm{G}_\Gamma^{\mathrm{OMF}} &= (1+n^2)\,\rho^2(1-(1+n^2)\,\rho_\sigma^2).
\end{aligned}\tag{4.3}$$

Thus, the coordinate curves $\sigma = \text{const.}$ and $\phi = \text{const.}$ are mutually orthogonal.

The unit normal vector in the Lorentzian sense is defined by

$$\mathbf{n}_\Gamma^{\mathrm{OMF}} = \frac{\Gamma_\sigma^{\mathrm{OMF}}\times\Gamma_\phi^{\mathrm{OMF}}}{\|\Gamma_\sigma^{\mathrm{OMF}}\times\Gamma_\phi^{\mathrm{OMF}}\|}.\tag{4.4}$$

Differentiating once more gives the coefficients of the second fundamental form:

$$\mathrm{L}_\Gamma^{\mathrm{OMF}} = \Im(\Gamma_{\sigma\sigma}^{\mathrm{OMF}},\mathbf{n}_\Gamma^{\mathrm{OMF}}),\quad \mathrm{M}_\Gamma^{\mathrm{OMF}} = \Im(\Gamma_{\sigma\phi}^{\mathrm{OMF}},\mathbf{n}_\Gamma^{\mathrm{OMF}}),\quad \mathrm{N}_\Gamma^{\mathrm{OMF}} = \Im(\Gamma_{\phi\phi}^{\mathrm{OMF}},\mathbf{n}_\Gamma^{\mathrm{OMF}}).\tag{4.5}$$

For the OMF embankment surface (3.4), the mixed coefficient $\mathrm{M}_\Gamma^{\mathrm{OMF}}$ vanishes due to coordinate orthogonality, and we have

$$\begin{aligned}
\mathrm{L}_\Gamma^{\mathrm{OMF}} &= -(1+n^2)(\rho\rho_{\sigma\sigma}+\rho_\sigma^2)\Im(\mathbf{T},\mathbf{n}_\Gamma^{\mathrm{OMF}})+\ \sqrt{1+n^2}\,\rho\rho_\sigma\kappa^2\Im(\mathbf{N},\mathbf{n}_\Gamma^{\mathrm{OMF}}),\\
\mathrm{N}_\Gamma^{\mathrm{OMF}} &= \pm\sqrt{1+n^2}\,\rho\sqrt{1-(1+n^2)\,\rho_\sigma^2}\,\Im(\cosh\phi\,\mathbf{B},\mathbf{n}_\Gamma^{\mathrm{OMF}}).
\end{aligned}\tag{4.6}$$

Consequently, the Gaussian curvature $\mathrm{K}_\Gamma^{\mathrm{OMF}}$ and the mean curvature $\mathrm{H}_\Gamma^{\mathrm{OMF}}$ are

$$\begin{aligned}
\mathrm{K}_\Gamma^{\mathrm{OMF}} &= \frac{\varepsilon\,(1+n^2)\,\rho_\sigma\rho_{\sigma\sigma}}{\rho(1-(1+n^2)\,\rho_\sigma^2)^2},\\
\mathrm{H}_\Gamma^{\mathrm{OMF}} &= \frac{(1+n^2)}{2\rho(1-(1+n^2)\,\rho_\sigma^2)^{3/2}}\Big[\rho_{\sigma\sigma}(1-(1+n^2)\,\rho_\sigma^2)-(1+n^2)\,\rho_\sigma^3\Big],
\end{aligned}\tag{4.7}$$

where $\varepsilon = 1$ for spacelike surface and $\varepsilon = -1$ for timelike surfaces.

Theorem 4.1. *Let* $\Gamma_{\beta}^{\mathrm{OMF}}(\sigma,\phi)$ *be the OMF embankment surface defined by* (3.4)*. Then the surface is* developable *if and only if*

$$\rho_{\sigma}\rho_{\sigma\sigma} = 0. \tag{4.8}$$

That is, the generating function $\rho(\sigma)$ *must be either constant or linear.*

Proof. From (4.7), $\mathrm{K}_{\Gamma}^{\mathrm{OMF}} = 0$ precisely when the numerator of its expression vanishes, since regularity implies $\rho_{\sigma}^2 < 1/(1+n^2)$. Hence, the condition $\rho_{\sigma}\rho_{\sigma\sigma} = 0$ characterizes developable cases, yielding either the constant ruling ($\rho = c$) or the linear form $\rho = a\sigma + b$. □

Theorem 4.2. *The OMF embankment surface* (3.4) *is minimal precisely when*

$$\rho_{\sigma\sigma}(1-(1+n^2)\rho_{\sigma}^2) - (1+n^2)\rho_{\sigma}^3 = 0. \tag{4.9}$$

Proof. Setting $\mathrm{H}_{\Gamma}^{\mathrm{OMF}} = 0$ in (4.7) leads directly to (4.9), as the prefactor remains nonzero for regular points. □

Remark 4.1. *The expressions* (4.7)–(4.9) *reveal that the curvature invariants of the OMF embankment surface depend explicitly on the derivatives of* $\rho(\sigma,\phi)$*, while implicitly involving the curvature* $\kappa(\sigma)$ *of the spine curve through the OMF coupling. Unlike Frenet or Darboux frame formulations, the OMF approach avoids twist instabilities and ensures smoother curvature variation under Lorentzian geometry.*

Theorem 4.3. *The OMF embankment surface* (3.4) *possesses a* constant mean curvature $\mathrm{H}_{\Gamma}^{\mathrm{OMF}} = \mathrm{H}_{0\Gamma}^{\mathrm{OMF}}$ *if and only if* $\rho(\sigma)$ *satisfies*

$$\rho_{\sigma\sigma}(1-(1+n^2)\rho_{\sigma}^2) - (1+n^2)\rho_{\sigma}^3 = 2\rho\mathrm{H}_{0\Gamma}^{\mathrm{OMF}}(1-(1+n^2)\rho_{\sigma}^2)^{3/2}/(1+n^2). \tag{4.10}$$

Proof. The result follows immediately by equating $\mathrm{H}_{\Gamma}^{\mathrm{OMF}}$ to the constant value $\mathrm{H}_{0\Gamma}^{\mathrm{OMF}}$ in (4.7) and rearranging. When $\mathrm{H}_{0\Gamma}^{\mathrm{OMF}} = 0$, it reduces to the minimal case in Theorem 4.2. □

4.1. OMF embankment-like and tubembankment-like surfaces

We now extend the previous formulation to two reduced surface classes derived from the general OMF embankment model, namely the OMF embankment-like surface and the OMF tubembankment-like surface. These are obtained by imposing constraints on the function $\rho(\sigma,\phi)$ according to the constancy of the ruling length.

Definition 4.1. Let $\beta(\sigma)$ be a regular spacelike curve in E_1^3 with the OMF triad $\{\mathbf{T}(\sigma),\mathbf{N}(\sigma),\mathbf{B}(\sigma)\}$. The OMF embankment-like surface is defined by

$$\begin{aligned}\Gamma_{\beta}^{\mathrm{OMF-L}}(\sigma,\phi) = {} & \beta(\sigma) - (1+n^2)\rho(\sigma)\rho_{\sigma}\mathbf{T}(\sigma) \pm \sqrt{1+n^2}\,\rho(\sigma)\sqrt{1-(1+n^2)\rho_{\sigma}^2}\,(\cosh\phi\,\mathbf{N}(\sigma) \\ & + \sinh\phi\,\mathbf{B}(\sigma)).\end{aligned} \tag{4.11}$$

If $\rho(\sigma) = c > 0$ is constant, the resulting surface is called the OMF tubembankment-like surface:

$$\Gamma_{T}^{\mathrm{OMF}}(\sigma,\phi) = \beta(\sigma) \pm c\sqrt{1+n^2}\,(\cosh\phi\,\mathbf{N}(\sigma) + \sinh\phi\,\mathbf{B}(\sigma)). \tag{4.12}$$

Theorem 4.4. *For the OMF embankment-like surface* (4.11)*, the Gaussian and mean curvatures are given by*

$$\begin{aligned} \mathrm{K}_{\Gamma}^{\mathrm{OMF-L}} &= \frac{\varepsilon\,(1+n^2)\,\rho_\sigma\rho_{\sigma\sigma}}{\rho(1-(1+n^2)\,\rho_\sigma^2)^2}, \\ \mathrm{H}_{\Gamma}^{\mathrm{OMF-L}} &= \frac{(1+n^2)}{2\rho(1-(1+n^2)\,\rho_\sigma^2)^{3/2}}\Big[\rho_{\sigma\sigma}(1-(1+n^2)\,\rho_\sigma^2)-(1+n^2)\,\rho_\sigma^3\Big]. \end{aligned} \tag{4.13}$$

Furthermore:

(1) The surface is developable ($\mathrm{K}_{\Gamma}^{\mathrm{OMF-L}}=0$*) if and only if* $\rho_\sigma\rho_{\sigma\sigma}=0$.
(2) The surface is minimal ($\mathrm{H}_{\Gamma}^{\mathrm{OMF-L}}=0$*) if and only if* $\rho_{\sigma\sigma}(1-(1+n^2)\,\rho_\sigma^2)=(1+n^2)\,\rho_\sigma^3$.

Proof. Since ρ depends solely on σ, the hyperbolic rotation parameter ϕ affects only the normal-plane orientation, ensuring that $\mathrm{F}_{\Gamma}^{\mathrm{OMF-L}}=\mathrm{M}_{\Gamma}^{\mathrm{OMF-L}}=0$. Inserting these relations into the curvature formulas yields (4.13), from which the developability and minimality conditions follow. □

Corollary 4.1. *If* $\rho(\sigma,\phi)=c>0$ *is constant, the OMF embankment surface reduces to the* OMF tubembankment-like surface

$$\Gamma_T^{\mathrm{OMF}}(\sigma,\phi)=\beta(\sigma)\pm c\,\sqrt{1+n^2}\,(\cosh\phi\,\mathbf{N}(\sigma)+\sinh\phi\,\mathbf{B}(\sigma)).$$

In this case, the Gaussian and mean curvatures are

$$\mathrm{K}_{\Gamma}^{\mathrm{OMF-TL}}=0, \qquad \mathrm{H}_{\Gamma}^{\mathrm{OMF-TL}}=\frac{\varepsilon}{c\,\sqrt{1+n^2}}, \tag{4.14}$$

and the surface is developable with constant mean curvature.

Proof. If $\rho(\sigma,\phi)=c>0$ is constant, then

$$\rho_\sigma=0, \qquad \rho_{\sigma\sigma}=0.$$

Substituting into the general expression of the Gaussian curvature (4.7), we obtain

$$\mathrm{K}_{\Gamma}^{\mathrm{OMF}}=\frac{\varepsilon(1+n^2)\,\rho_\sigma\rho_{\sigma\sigma}}{\rho(1-(1+n^2)\rho_\sigma^2)^2}=0,$$

so the surface is developable.

However, substituting directly into the mean curvature formula (4.7) leads to an indeterminate form. Therefore, we compute the mean curvature from its definition

$$\mathrm{H}_{\Gamma}^{\mathrm{OMF}}=\frac{E_{\Gamma}^{\mathrm{OMF}}N_{\Gamma}^{\mathrm{OMF}}+G_{\Gamma}^{\mathrm{OMF}}L_{\Gamma}^{\mathrm{OMF}}-2F_{\Gamma}^{\mathrm{OMF}}M_{\Gamma}^{\mathrm{OMF}}}{2(E_{\Gamma}^{\mathrm{OMF}}G_{\Gamma}^{\mathrm{OMF}}-F_{\Gamma}^{\mathrm{OMF}^2})}.$$

For the parametrization

$$\Gamma_T^{\mathrm{OMF}}(\sigma,\phi)=\beta(\sigma)\pm c\,\sqrt{1+n^2}\,(\cosh\phi\,\mathbf{N}(\sigma)+\sinh\phi\,\mathbf{B}(\sigma)),$$

a direct computation shows that the coordinate curves are orthogonal, hence $F=0$ and $M=0$. The first fundamental coefficients E and G remain nonzero, while the second fundamental coefficients reduce

to constant contributions determined by the Lorentzian geometry of the normal section. Consequently, the mean curvature simplifies to

$$\mathrm{H}_{\Gamma}^{\mathrm{OMF-TL}} = \frac{\varepsilon}{c\sqrt{1+n^2}},$$

which is constant. Therefore, the OMF tubembankment–like surface is developable with constant mean curvature. □

5. Illustrative examples and applications

In this section, we present a series of illustrative examples to demonstrate the effectiveness and applicability of the proposed OMF in the construction and analysis of ruled surfaces in Minkowski 3-space. These examples are designed to highlight the geometric behavior of the associated surfaces, as well as to emphasize the computational advantages and stability of the OMF in comparison with classical frame formulations.

Example 5.1. *We begin by considering a spacelike helical curve in the Minkowski 3-space* E_1^3*, endowed with the Lorentzian metric*

$$\Im(x, y, z) = x^2 + y^2 - z^2.$$

Let $\beta(\sigma)$ *be defined by*

$$\begin{aligned} \beta(\sigma) &= (\cos\sigma,\ \sin\sigma,\ a\sigma), \\ \beta'(\sigma) &= (-\sin\sigma,\ \cos\sigma,\ a), \\ \beta''(\sigma) &= (-\cos\sigma,\ -\sin\sigma,\ 0), \end{aligned} \tag{5.1}$$

where $a \in \mathbb{R}$ *represents the pitch parameter of the helix.*

The Lorentzian norm of the tangent vector is given by

$$\Im(\beta'(\sigma), \beta'(\sigma)) = 1 - a^2.$$

Thus, the curve β *is spacelike whenever* $a^2 < 1$*, and becomes timelike for* $a^2 > 1$*. In our case, we take* $a = 0.4$*. Then the associated Frenet trihedron* (t, n, b) *is*

$$\begin{aligned} t(\sigma) &= (-0.929\ \sin\sigma,\ 0.929\ \cos\sigma,\ 0.371), \\ n(\sigma) &= (-\cos\sigma,\ -\sin\sigma,\ 0), \\ b(\sigma) &= (0.371\ \sin\sigma,\ -0.371\ \cos\sigma,\ 0.929), \end{aligned}$$

with curvature and torsion values

$$\kappa = 0.893, \qquad \tau = 0.345.$$

The corresponding OMF is

$$\begin{aligned} \mathbf{T}(\sigma) &= (-0.929\ \sin\sigma,\ 0.929\ \cos\sigma,\ 0.371), \\ \mathbf{N}(\sigma) &= (-\cos\sigma,\ -\sin\sigma,\ 0), \\ \mathbf{B}(\sigma) &= (0.371\ \sin\sigma,\ -0.371\ \cos\sigma,\ 0.929). \end{aligned} \tag{5.2}$$

Let $n > 0$ denote the Lorentzian slope factor and $\rho(\sigma)$ a differentiable scalar function specifying the ruling length along the surface. The parametric form of the general OMF embankment surface is expressed as

$$\begin{aligned}\Gamma_{\beta}^{\mathrm{OMF}}(\sigma,\phi) &= \beta(\sigma) - (1+n^2)\,\rho(\sigma)\rho_{\sigma}\,\mathbf{T}(\sigma)\\ &\pm \sqrt{1+n^2}\,\rho(\sigma)\sqrt{1-(1+n^2)\,\rho_{\sigma}^2}\,(\cosh\phi\,\mathbf{N}(\sigma)+\sinh\phi\,\mathbf{B}(\sigma)).\end{aligned} \tag{5.3}$$

For any surface of the form (5.3)*, the Gaussian curvature $\mathrm{K}_{\Gamma}^{\mathrm{OMF}}(\sigma)$ and mean curvature $\mathrm{H}_{\Gamma}^{\mathrm{OMF}}(\sigma)$ are determined by*

$$\begin{aligned}\mathrm{K}_{\Gamma}^{\mathrm{OMF}}(\sigma) &= \frac{\varepsilon(1+n^2)\,\rho_{\sigma}\rho_{\sigma\sigma}}{\rho(1-(1+n^2)\,\rho_{\sigma}^2)^2},\\ \mathrm{H}_{\Gamma}^{\mathrm{OMF}}(\sigma) &= \frac{(1+n^2)}{2\rho(1-(1+n^2)\,\rho_{\sigma}^2)^{3/2}}\Big[\rho_{\sigma\sigma}(1-(1+n^2)\,\rho_{\sigma}^2)-(1+n^2)\,\rho_{\sigma}^3\Big],\end{aligned} \tag{5.4}$$

where $\varepsilon = 1$ for the spacelike case.

For illustration, consider $n = 0.5$, $\rho(\sigma) = 0.5 + 0.2\sin\sigma$. Then (see Figure 1),

$$\begin{aligned}\Gamma_{\beta}^{\mathrm{OMF}}(\sigma,\phi) &= (\cos\sigma,\ \sin\sigma,\ 0.4\sigma) - 0.25(0.5+0.2\sin\sigma)(-\sin\sigma,\ \cos\sigma,\ 0.4)\\ &\pm 1.118(0.5+0.2\sin\sigma)\sqrt{1-0.05\cos^2\sigma}\\ &\times\Big[\cosh\phi\,(-\cos\sigma,\ -\sin\sigma,\ 0)+\sinh\phi\,(0.371\sin\sigma,\ -0.371\cos\sigma,\ 0.929)\Big].\end{aligned} \tag{5.5}$$

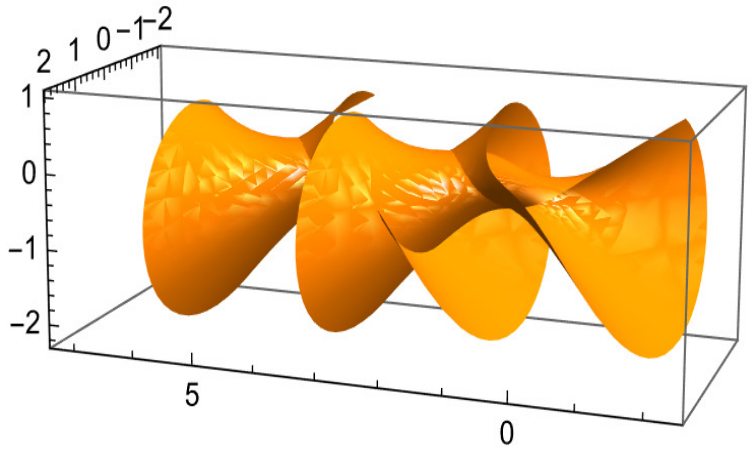

Figure 1. OMF embankment surface $\Gamma_{\beta}^{\mathrm{OMF}}(\sigma,\phi)$ with parameter ranges $\sigma \in [0, 2\pi]$ and $\phi \in [-1, 1]$. The horizontal axis corresponds to the parameter σ, while the vertical variation is governed by ϕ.

The corresponding curvature expressions are found to be (see Figures 2 and 3),

$$\begin{aligned}\mathrm{K}_{\Gamma}^{\mathrm{OMF}}(\sigma) &= \frac{-0.025\,\varepsilon\,\sin(2\sigma)}{(0.5+0.2\sin\sigma)(1-0.05\cos^2\sigma)^2},\\ \mathrm{H}_{\Gamma}^{\mathrm{OMF}}(\sigma) &= -\frac{1.25\Big[0.2\,\sin\sigma(1-0.05\,\cos^2\sigma)+0.01\,\cos^3\sigma\Big]}{2(0.5+0.2\sin\sigma)(1-0.05\,\cos^2\sigma)^{3/2}}.\end{aligned} \tag{5.6}$$

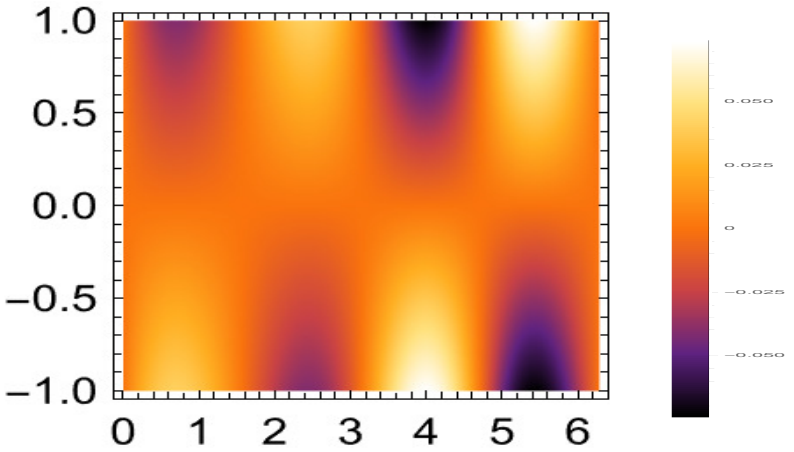

Figure 2. Distribution of $K_{\Gamma}^{OMF}(\sigma)$ on the non developable OMF embankment surface.

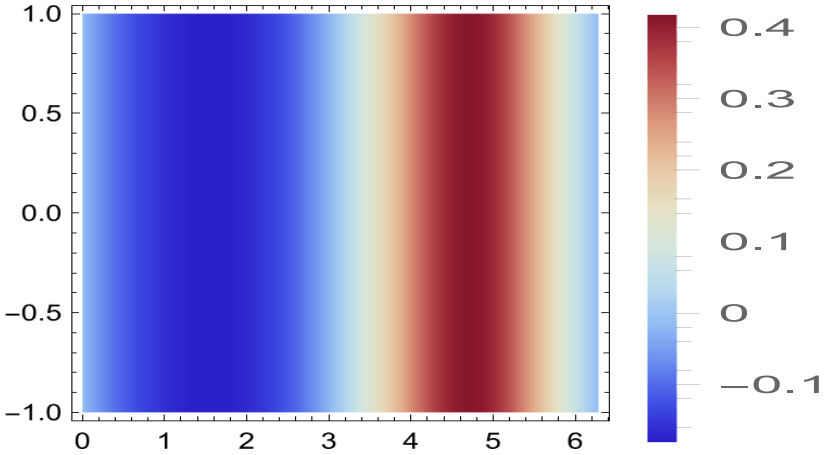

Figure 3. Distribution of $H_{\Gamma}^{OMF}(\sigma)$ on the non developable OMF embankment surface.

Next, assuming a ϕ-dependent ruling function with $n = 0.5$, $\rho(\sigma) = 0.4 + 0.1\sigma$, $\rho_{\sigma} = 0.1$, and $\rho_{\sigma\sigma} = 0$, the OMF embankment-like surface is expressed by (see Figure 4)

$$\Gamma_{\beta}^{OMF-L}(\sigma,\phi) = \beta(\sigma) - 0.125(0.4 + 0.1\sigma)\mathbf{T}(\sigma) \pm 1.118(0.4 + 0.1\sigma)\Big[\cosh\phi\,\mathbf{N}(\sigma) + \sinh\phi\,\mathbf{B}(\sigma)\Big].$$

Substituting the frame explicitly gives

$$\begin{aligned}\Gamma_{\beta}^{OMF-L}(\sigma,\phi) = {} & (\cos\sigma,\ \sin\sigma,\ 0.4\sigma) - 0.125(0.4 + 0.1\sigma)(-\sin\sigma,\ \cos\sigma,\ 0.4) \\ & \pm 1.118(0.4 + 0.1\sigma)\Big[\cosh\phi(-\cos\sigma, -\sin\sigma, 0) \\ & + \sinh\phi(0.371\sin\sigma, -0.371\cos\sigma, 0.929)\Big].\end{aligned} \tag{5.7}$$

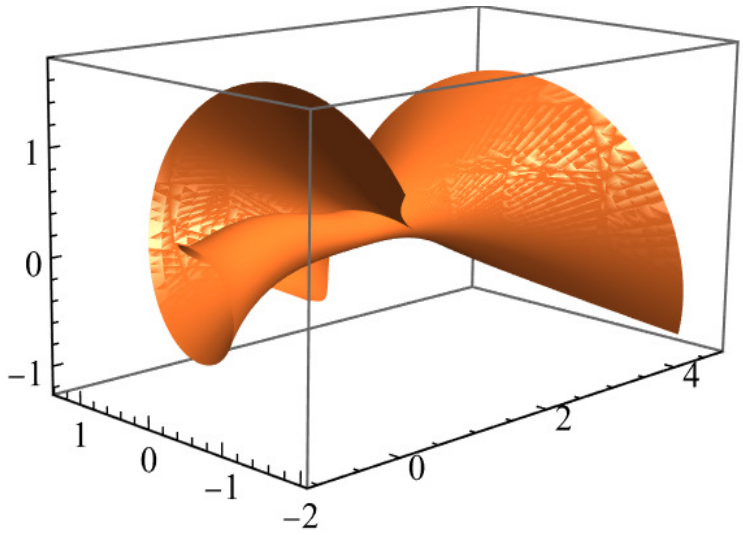

Figure 4. OMF embankment–like surface $\Gamma_{\beta}^{\mathrm{OMF-L}}(\sigma,\phi)$.

From this model it follows that $\mathrm{K}_{\Gamma}^{\mathrm{OMF-L}} = 0$, *while the mean curvature remains nonzero, corresponding to a developable ruled surface with (see Figure 5)*

$$\begin{aligned}
\mathrm{H}_{\Gamma}^{\mathrm{OMF-L}}(\sigma) &= \frac{(1+n^2)}{2\rho(\sigma)\left(1-(1+n^2)\rho_{\sigma}^2\right)^{3/2}}\left[\rho_{\sigma\sigma}\left(1-(1+n^2)\rho_{\sigma}^2\right)-(1+n^2)\rho_{\sigma}^3\right] \\
&= \frac{1.25}{2(0.4+0.1\sigma)\left(1-1.25\times 0.01\right)^{3/2}}\left[0\cdot(1-0.0125)-1.25\times(0.1)^3\right] \\
&= \frac{1.25}{2(0.4+0.1\sigma)\,(0.9875)^{3/2}}\left[-1.25\times 0.001\right] = -\frac{1.5625\times 10^{-3}}{2(0.4+0.1\sigma)\,(0.9875)^{3/2}} \\
&\approx -\frac{1.5625\times 10^{-3}}{1.963\,(0.4+0.1\sigma)}.
\end{aligned}$$

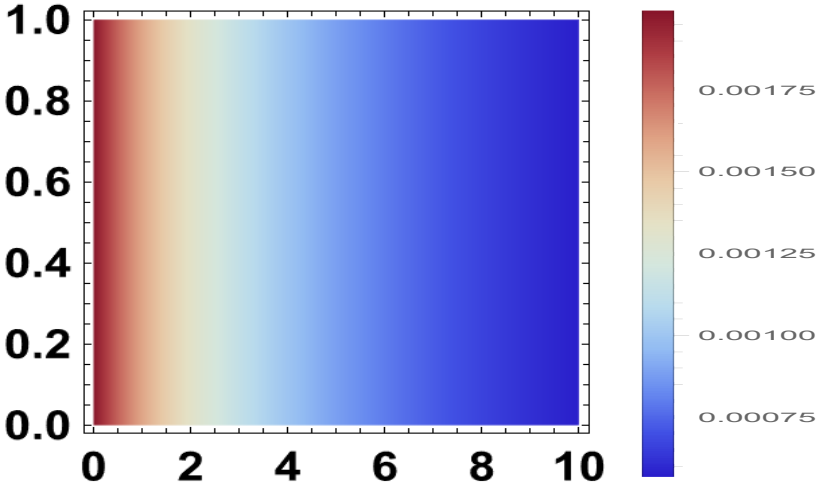

Figure 5. Distribution of $\mathrm{H}_{\Gamma}^{\mathrm{OMF-L}}(\sigma)$ on the developable OMF embankment surface.

Finally, for the constant case $\rho(\sigma) = 0.6$, the corrected tubembankment-like surface becomes

$$\Gamma_T^{\mathrm{OMF}}(\sigma,\phi) = \beta(\sigma) \pm 0.671\Big[\cosh\phi\,\mathbf{N}(\sigma) + \sinh\phi\,\mathbf{B}(\sigma)\Big].$$

Expanding explicitly, we obtain the corrected form (see Figure 6)

$$\Gamma_T^{\mathrm{OMF}}(\sigma,\phi) = \begin{pmatrix} \cos\sigma \mp 0.671[\cosh\phi\,\cos\sigma - 0.371\sinh\phi\,\sin\sigma] \\ \sin\sigma \mp 0.671[\cosh\phi\,\sin\sigma + 0.371\sinh\phi\,\cos\sigma] \\ 0.4\sigma \mp 0.671\times 0.929\sinh\phi \end{pmatrix}. \tag{5.8}$$

This surface represents a Lorentzian cylindrical form generated by the helical curve $\beta(\sigma)$, satisfying

$$\mathrm{K}_\Gamma^{\mathrm{OMF-TL}} = 0, \qquad \mathrm{H}_\Gamma^{\mathrm{OMF-TL}}(\sigma) \approx 1.491\,\varepsilon,$$

indicating a developable surface with constant mean curvature.

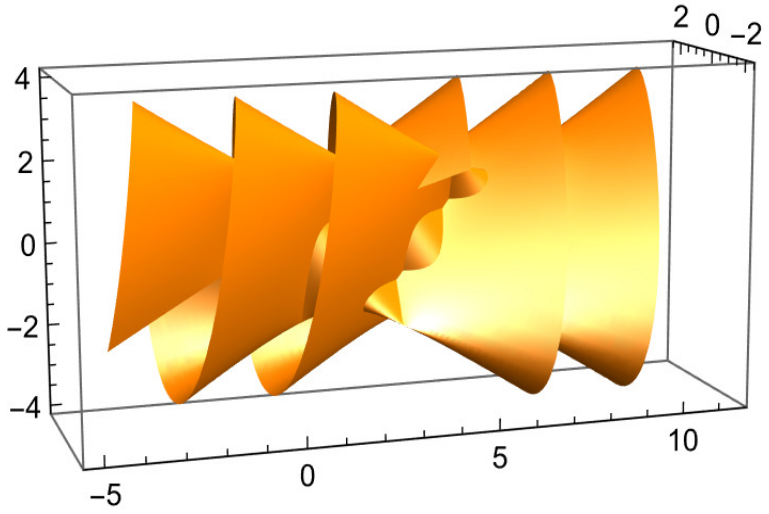

Figure 6. OMF tubembankment-like surface $\Gamma_T^{\mathrm{OMF}}(\sigma,\phi)$.

Example 5.2. *In this example, we illustrate the failure of the classical Frenet frame at points where the curvature vanishes and demonstrate that the OMF remains well-defined. Moreover, we construct the associated OMF embankment surface and analyze its geometric properties.*

Consider the spacelike curve in Minkowski 3-space E_1^3 defined by

$$\beta(\sigma) = (\sigma,\ \sigma^3,\ 0). \tag{5.9}$$

Its derivatives are

$$\beta'(\sigma) = (1,\ 3\sigma^2,\ 0), \qquad \beta''(\sigma) = (0,\ 6\sigma,\ 0).$$

The Lorentzian norm satisfies

$$\Im(\beta',\beta') = 1 + 9\sigma^4 > 0,$$

so the curve is spacelike. The unit tangent vector is

$$t(\sigma) = \frac{(1, 3\sigma^2, 0)}{\sqrt{1+9\sigma^4}}.$$

The curvature is

$$\kappa(\sigma) = \frac{|6\sigma|}{(1+9\sigma^4)^{3/2}}, \quad \textit{hence} \quad \kappa(0) = 0.$$

Thus, at $\sigma = 0$*, the normal vector*

$$n(\sigma) = \frac{t'(\sigma)}{\|t'(\sigma)\|}$$

is undefined, and the Frenet frame fails.

Now, let $\mathbf{E} = (0, 0, 1)$*. Then*

$$\mathbf{N}(\sigma) = \frac{\mathbf{E} - \langle \mathbf{E}, \mathbf{T}\rangle \mathbf{T}}{\|\mathbf{E} - \langle \mathbf{E}, \mathbf{T}\rangle \mathbf{T}\|}, \qquad \mathbf{B}(\sigma) = \mathbf{T}(\sigma) \times \mathbf{N}(\sigma).$$

This frame remains smooth for all σ*, including* $\sigma = 0$ *(see Table 2).*

Table 2. Comparison between Frenet frame and OMF.

Property	Frenet frame	OMF
Depends on curvature	Yes	No
Defined at $\kappa = 0$	No	Yes
Continuity	Discontinuous	Smooth
Stability	Low	High

Let $n = 0.25$ *and* $\rho(\sigma) = 0.25 + 0.5\cos\sigma$*. Then* $1 + n^2 = 1.0625$*,* $\sqrt{1+n^2} \approx 1.031$*,* $\rho_\sigma = -0.5\sin\sigma$*, and* $\rho_{\sigma\sigma} = -0.5\cos\sigma$*. Then, the surface becomes (see Figures 7–9):*

$$\begin{aligned} \Gamma_\beta^{\mathrm{OMF}}(\sigma, \phi) = \beta(\sigma) &+ 0.53125(0.25 + 0.5\cos\sigma)\sin\sigma\, \mathbf{T}(\sigma) \\ &\pm 1.031(0.25 + 0.5\cos\sigma)\sqrt{1 - 0.265625\sin^2\sigma} \\ &\times \Big(\cosh\phi\, \mathbf{N}(\sigma) + \sinh\phi\, \mathbf{B}(\sigma)\Big), \end{aligned} \tag{5.10}$$

and

$$\begin{aligned} \mathrm{K}_\Gamma^{\mathrm{OMF}}(\sigma) &= \frac{1.0625\,\varepsilon\,(-0.5\sin\sigma)(-0.5\cos\sigma)}{(0.25 + 0.5\cos\sigma)(1 - 0.265625\sin^2\sigma)^2} \\ &= \frac{0.265625\,\varepsilon\,\sin\sigma\cos\sigma}{(0.25 + 0.5\cos\sigma)(1 - 0.265625\sin^2\sigma)^2} \\ &= \frac{0.1328125\,\varepsilon\,\sin(2\sigma)}{(0.25 + 0.5\cos\sigma)(1 - 0.265625\sin^2\sigma)^2}, \end{aligned} \tag{5.11}$$

$$\begin{aligned} \mathrm{H}_\Gamma^{\mathrm{OMF}}(\sigma) &= \frac{1.0625}{2(0.25 + 0.5\cos\sigma)(1 - 0.265625\sin^2\sigma)^{3/2}} \\ &\quad \times \Big[(-0.5\cos\sigma)(1 - 0.265625\sin^2\sigma) - 1.0625(-0.5\sin\sigma)^3\Big] \\ &= -\frac{1.0625}{2(0.25 + 0.5\cos\sigma)(1 - 0.265625\sin^2\sigma)^{3/2}} \\ &\quad \times \Big[0.5\cos\sigma(1 - 0.265625\sin^2\sigma) - 0.1328125\sin^3\sigma\Big]. \end{aligned} \tag{5.12}$$

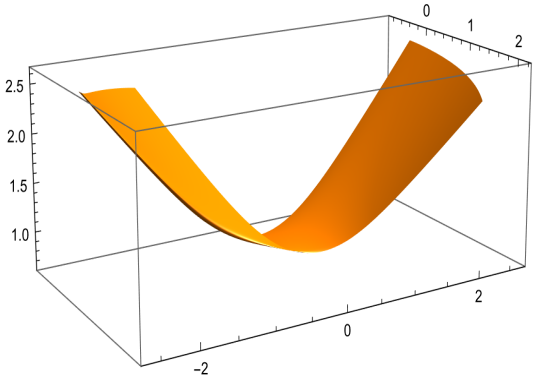

Figure 7. OMF embankment surface $\Gamma_{\beta}^{\mathrm{OMF}}(\sigma, \phi)$ with parameter ranges $\sigma \in [0, \frac{\pi}{6}]$ and $\phi \in [-2, 2]$. The horizontal axis corresponds to the parameter σ, while the vertical variation is governed by ϕ.

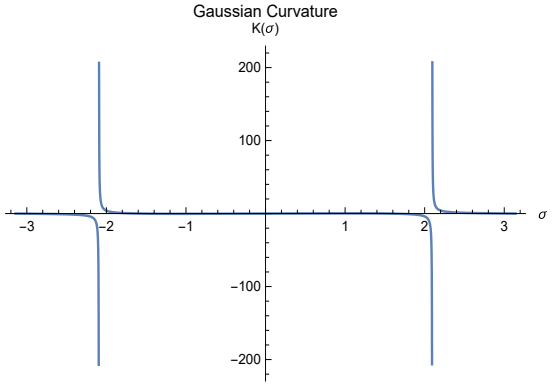

Figure 8. Distribution of the Gaussian curvature $\mathrm{K}_{\Gamma}^{\mathrm{OMF}}(\sigma)$ for the OMF embankment surface near the inflection region. The curvature varies with σ and changes sign, indicating the presence of alternating elliptic and hyperbolic regions along the surface.

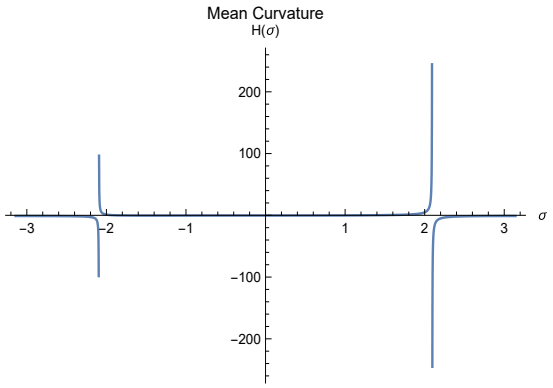

Figure 9. Distribution of the mean curvature $\mathrm{H}_{\Gamma}^{\mathrm{OMF}}(\sigma)$ for the OMF embankment surface. The curvature remains smooth across the inflection point, confirming the regularity of the OMF-based construction even where the Frenet frame becomes undefined.

This example confirms that the Frenet frame becomes singular at $\sigma = 0$, while the OMF remains smooth. The resulting embankment surface is well-defined and exhibits nontrivial curvature behavior governed by trigonometric variations of σ.

6. Conclusions

This work presents a unified formulation for embankment-type ruled surfaces in the Lorentzian space E_1^3 based on the OMF. The proposed approach provides a stable and geometrically consistent alternative to classical constructions, overcoming limitations associated with Darboux and rotation minimizing frames, particularly in the presence of torsion irregularities.

It is important to stress that the present formulation is not merely an extension of classical Euclidean constructions, but rather a structurally different approach adapted to the Lorentzian metric of E_1^3. In this context, the indefinite inner product necessitates explicit consideration of the causal character of vectors and curves, which directly influences the resulting surface geometry. The OMF $\{\mathbf{T}, \mathbf{N}, \mathbf{B}\}$ ensures a metric-compatible orthogonal system that remains well-defined even in situations where traditional Euclidean frames may lose regularity. Moreover, the surface generation is based on the envelope of a one-parameter family of Lorentzian cones aligned with the tangent vector $\mathbf{T}(\sigma)$, producing hyperbolic variations governed by $\cosh\varphi$ and $\sinh\varphi$, rather than circular rotations. Consequently, the curvature quantities K_Γ^{OMF} and H_Γ^{OMF} arise intrinsically from the Lorentzian structure and depend on the differential behavior of the ruling function $\rho(\sigma)$, leading to developability and minimality conditions that differ essentially from their Euclidean analogues.

Explicit parametrizations of the OMF embankment surface were derived via the envelope of Lorentzian cone families, allowing direct computation of the fundamental forms and curvature invariants. In contrast to earlier studies (e.g., [2]), where constructions rely on Euclidean or partially adapted frames, the present method yields closed-form expressions that remain valid under the Lorentzian metric without degeneracy. In particular, the Gaussian and mean curvatures are expressed explicitly in terms of the ruling function $\rho(\sigma)$ and its derivatives, providing a transparent link between geometric behavior and analytic structure.

The analysis further establishes precise criteria for key geometric properties: The surface is developable if and only if $\rho_\sigma \rho_{\sigma\sigma} = 0$, while minimality and constant mean curvature conditions are characterized through nonlinear differential relations. These results extend classical criteria to a genuinely Lorentzian setting and unify the treatment of minimal and constant mean curvature surfaces within a single framework.

Special subclasses, including the OMF embankment-like and tubembankment-like surfaces, illustrate the adaptability of the model. In particular, the constant-radius case yields a developable surface with constant mean curvature

$$H_\Gamma^{\text{OMF-TL}} = \frac{\varepsilon}{c\sqrt{1+n^2}},$$

highlighting the emergence of Lorentzian cylindrical structures as natural limit configurations.

Overall, the OMF framework provides a robust tool for the geometric modeling of ruled surfaces in non-Euclidean environments, combining analytical tractability with structural stability. Future work may explore extensions to timelike and lightlike geometries, higher-dimensional Minkowski spaces, and applications in kinematic design, relativistic modeling, and computer-aided geometric design.

Author contributions

Mona Bin-Asfour: Writing–review & editing, visualization, validation, supervision, software, methodology, formal analysis, conceptualization, funding acquisition; Ahmed Ghaliah Alhamzi: Writing–original draft, validation, software, resources, methodology, investigation, formal analysis; Emad Solouma: Writing–review & editing, visualization, validation, formal analysis, data curation, conceptualization; Sayed Saber: Writing–review & editing, supervision. All authors have read and approved the final version of the manuscript for publication.

Use of Generative-AI tools declaration

The authors declare they have not used Artificial Intelligence (AI) tools in the creation of this article.

Acknowledgements

This work was supported and funded by the Deanship of Scientific Research at Imam Mohammad Ibn Saud Islamic University (IMSIU) (grant number IMSIU-DDRSP2601).

Conflicts of interest

The authors declare no conflicts of interest in this paper.

References

1. A. A. Almoneef, R. A. Abdel-Baky, Timelike constant axis ruled surface family in Minkowski 3-space, *Symmetry*, **16** (2024), 677. https://doi.org/10.3390/sym16060677
2. M. T. Aldossary, R. A. Abdel-Baky, Sweeping surface due to the rotation minimizing Darboux frame in Euclidean 3-space E^3, *AIMS Mathematics*, **8** (2023), 447–462. https://doi/10.3934/math.2023021
3. A. A. Almoneef, R. A. Abdel-Baky, Slant spacelike ruled surfaces and their Bertrand offsets, *Front. Phys.*, **12** (2024), 1484936. https://doi.org/10.3389/fphy.2024.1484936
4. M. P. do Carmo, *Differential geometry of curves and surfaces: Revised and updated second edition*, Dover Publications, 2016.
5. H. Ceyhan, Z. B. Özdemir, I. Gök, Multiplicative generalized tube surfaces with multiplicative quaternion algebra, *Math. Methods Appl. Sci.*, **47** (2024), 9157–9168. https://doi.org/10.1002/mma.10065
6. H. B. Çolakoğlu, İ. Öztürk, O. Çelik, M. Özdemir, Generalized Galilean rotations, *Symmetry*, **16** (2024), 1553. https://doi.org/10.3390/sym16111553
7. E. Damar, A novel approach to ruled surfaces using Adjoint curve, *Symmetry*, **17** (2025), 1018. https://doi.org/10.3390/sym17071018
8. H. K. Elsayied, A. A. Altaha, A. Elsharkawy, On some special curves according to the modified orthogonal frame in Minkowski 3-space E_1^3, *Kasmera*, **49** (2021), 2–15.

9. A. Elsharkawy, Y. Tashkandy, W. Emam, C. Cesarano, N. Elsharkawy, On some quasi-curves in Galilean three-space, *Axioms*, **12** (2023), 823. https://doi.org/10.3390/axioms12090823
10. A. Elsharkawy, N. Elsharkawy, Quasi-position vector curves in Galilean 4-space, *Front. Phys.*, **12** (2024), 1400730. https://doi.org/10.3389/fphy.2024.1400730
11. K. Eren, H. H. Kosal, Evolution of space curves and the special ruled surfaces with modified orthogonal frame, *AIMS Mathematics*, **5** (2020), 2027–2039. https://doi.org/10.3934/math.2020134
12. S. Gaber, A. Al Elaiw, Evolution of null Cartan and pseudo null curves via the Bishop frame in Minkowski space $R^{2,1}$, *AIMS Mathematics*, **10** (2025), 3691–3709. https://doi.org/10.3934/math.2025171
13. I. Golgeleyen, Y. Yayli, E. Y. Bulgan, Developable ruled surfaces with constant mean curvature along a curve, *Mathematics*, **14** (2026), 234. https://doi.org/10.3390/math14020234
14. E. Kocakuşaklı, Embankment surfaces with the Darboux frame in Euclidean 3-space, *AIMS Mathematics*, **10** (2025), 20979–21003. https://doi.org/10.3934/math.2025937
15. Y. Li, Z. Chen, S. H. Nazra, R. A. Abdel-Baky, Singularities for timelike developable surfaces in Minkowski 3-space, *Symmetry*, **15** (2023), 277. https://doi.org/10.3390/sym15020277
16. R. López, Differential geometry of curves and surfaces in Lorentz-Minkowski space, *Int. Electron. J. Geom.*, **7** (2014), 44–107.
17. Y. Li, A. Çalışkan, Quaternionic shape operator and rotation matrix on ruled surfaces, *Axioms*, **12** (2023), 486. https://doi.org/10.3390/axioms12050486
18. Y. Li, H. S. Abdel-Aziz, H. M. Serry, F. M. El-Adawy, M. K. Saad, Geometric visualization of evolved ruled surfaces via alternative frame in Lorentz-Minkowski 3-space, *AIMS Mathematics*, **9** (2024), 25619–25635. https://doi.org/10.3934/math.20241251
19. F. Massamba, S. Ssekajja, A geometric flow on null hypersurfaces of Lorentzian manifolds, *Topol. Algebra Appl.*, **10** (2022), 185–195. https://doi.org/10.1515/taa-2022-0126
20. W. M. Mahmoud, E. M. Mohameda, M. Soliman, Investigate and designing translation surface with a 2-Bishop frame in the Galilean space, *Aswan Sci. Technol. Bull.*, 2023.
21. M. Messaoudi, M. Marin, N. E. Taha, G. S. Al-Mutairi, S. Saber, Higher-dimensional geometry and singularity structure of osculating type-II ruled surfaces in Lorentzian spaces, *Mathematics*, **14** (2026), 263. https://doi.org/10.3390/math14020263
22. B. O'Neill, *Semi-Riemannian geometry with applications to relativity*, New York: Academic Press, 1983.
23. K. Orbay, D. Aydoğan, T. Şahin, Ruled invariants and ruled surfaces created with spherical curves in Galilean space, *BEU Fen Bilimleri Dergisi*, **15** (2026), 394–407. https://doi.org/10.17798/bitlisfen.1824791
24. V. H. Patty-Yujra, G. Ruiz-Hernández, Timelike surfaces in Minkowski space with a canonical null direction, *J. Geom.*, **109** (2018), 35. https://doi.org/10.1007/s00022-018-0434-2
25. G. S. Silva, V. Silva, Classification of ruled surfaces as homothetic self-similar solutions of the inverse mean curvature flow in Lorentz-Minkowski 3-space, *Bull. Braz. Math. Soc. New Series*, **54** (2023), 48. https://doi.org/10.1007/s00574-023-00364-6

26. E. Solouma, I. Al-Dayel, M. A. Khan, M. Abdelkawy, Investigation of special type-II Smarandache ruled surfaces due to the rotation minimizing Darboux frame in E^3, *Symmetry*, **15** (2023), 2207. https://doi.org/10.3390/sym15122207

27. E. Solouma, I. Al-Dayel, M. A. Khan, Y. A. A. Lazer, Characterization of imbricate-ruled surfaces via rotation-minimizing Darboux frame in Minkowski 3-space E_1^3, *AIMS Mathematics*, **9** (2024), 13028–13042. https://doi.org/10.3934/math.2024635

28. E. Solouma, S. Saber, H. M. Baskonus, Exploring harmonic evolute geometries derived from tubular surfaces in Minkowski 3-space using the RM Darboux frame, *Mathematics*, **13** (2025), 2329. https://doi.org/10.3390/math13152329

29. E. Solouma, I. Al-Dayel, M. A. Abdelkawy, Ruled surfaces and their geometric invariants via the orthogonal modified frame in Minkowski 3-space, *Mathematics*, **13** (2025), 940. https://doi.org/10.3390/math13060940

30. E. Solouma, G. Alhamzi, M. Bin-Asfour, S. Saber, Unified curvature modeling of surface constrained helices and associated ruled surfaces, *AIMS Mathematics*, **11** (2026), 7847–7870. http://dx.doi.org/10.3934/math.2026324

31. D. J. Struik, *Lectures on classical differential geometry*, 2 Eds., Dover Publications, 1988.

32. D. W. Yoon, Z. Yüzbaşı, E. C. Aslan, Evolution of space-like curves and special time-like ruled surfaces in Minkowski space, *Indian J. Phys.*, **96** (2022), 995–999. https://doi.org/10.1007/s12648-021-02021-4

AIMS Press